II. Table II shows all of the energy levels involved in the calculation, while Fig. 10 shows only those levels that are pertinent to the experiment.

Fairly large deviations between the experimental and theoretical levels are shown in Fig. 10. The calculated effects of configuration mixing are not large enough to move the $J=2$ levels apart as much as is indicated by the experiment. This discrepancy between the experiment and the calculation also appears in a comparison of values of S for the first-excited state. The experimental value of S is 1.4, while the calculated value is 1.9. The results for the ground state are similar, but the errors on the experimental value of S are large for this case.

PHYSICAL REVIEW VOLUME 125, NUMBER 3 FEBRUARY 1, 1962

Low-Resolution Survey of (d,α) Reactions in Heavy Nuclei*

JAMES B. MEAD AND BERNARD L. COHEN
University of Pittsburgh, Pittsburgh, Pennsylvania
(Received August 2, 1961)

A low-resolution survey of (d,α) reactions was made for about 28 heavy nuclei between $Z=28$ and $Z=83$ with an incident deuteron energy of 15 Mev. Energy distributions and cross sections were obtained at scattering angles of 30°, 60°, 90°, and 120°. The observed energy spectra are characterized by two strong peaks which vary regularly in energy and cross section with atomic weight. Energy distributions and cross sections of the low-energy peak are in accord with statistical theory. The principal features of the high-energy peak can be explained with the assumption of a process which involves the pickup of a proton and neutron from separate single-particle states.

INTRODUCTION

NUCLEAR reaction experiments are usually performed with two aims in mind: to study the reaction mechanism, and to gain insight into the problem of nuclear structure. Of particular interest are the energy distributions of the reaction products emitted at various scattering angles. From these data it is often possible to determine whether the reaction mechanism is direct in nature or whether it proceeds through the intermediate stage of a compound nucleus. It is also often possible to distinguish between various types of direct interactions and to determine parameters related to the reaction mechanism.

Previous experiments involving (d,α) reactions are notably sparse, except for some detailed work on light nuclei.[1–4] To date, the heavy-element region $(A>60)$ has been almost completely neglected. In view of this fact, it was decided to make a low-resolution survey of energy distributions and cross sections at several scattering angles for about 28 nuclei between mass numbers 59 and 209. Preliminary results for this experiment have appeared in a previous note.[5]

EXPERIMENTAL TECHNIQUES

Fifteen-Mev deuterons that initiated reactions studied in this experiment were obtained from the University of Pittsburgh cyclotron. The incident beam was momentum analyzed and contained a resultant energy spread of about 80 kev. The associated scattering system has been discussed in detail by previous workers[6–8] and will not be treated here. Beam current was collected by a Faraday cup; the accumulated charge was measured by a precision current integrator with an error less than 1%.

The detectors consisted of a CsI crystal scintillator and proportional counter used in coincidence as a $(dE/dX)-E$ particle separation system.[9] Pulses from each of the detectors were separately analyzed by single-channel pulse-height selectors (PHS) used as integral discriminators. The PHS outputs were presented to a coincidence circuit which subsequently gated a 256-channel analyzer (refer to Fig. 1). By proper setting of the PHS discrimination level associated with the (dE/dX) (proportional) counter, less ionizing reaction products could be rejected in favor of the remaining alphas.

As a result of the high Q values inherent in (d,α) reactions and the large Coulomb barriers for alphas, the spectra of outgoing particles were limited to an energy region where energy loss does not change rapidly with energy. In almost all cases the entire alpha energy spectrum could be obtained with a single PHS discriminator setting, thus obviating the need for a pulse

* This work was done at Sarah Mellon Scaife Radiation Laboratory and supported by the National Science Foundation.
[1] G. E. Fischer and V. K. Fischer, Phys. Rev. **114**, 533 (1959).
[2] F. Pellegrini (to be published).
[3] Chuin Hu, J. Phys. Soc. Japan **15**, 1741 (1960).
[4] N. Cindro, M. Cerineo, and A. Strazalkowski, Nuclear Phys. **24**, 107 (1961).
[5] J. B. Mead and B. L. Cohen, Phys. Rev. Letters **5**, 105 (1960).
[6] R. S. Bender, E. M. Reilly, A. J. Allen, R. Ely, J. S. Arthur, and H. J. Hausman, Rev. Sci. Instr. **23**, 542 (1952).
[7] S. H. Levine, Ph.D. thesis, University of Pittsburgh, 1953 (unpublished).
[8] W. E. Moore, Ph.D. thesis, University of Pittsburgh, 1959 (unpublished).
[9] F. A. Aschenbrenner, Phys. Rev. **98**, 657 (1955).

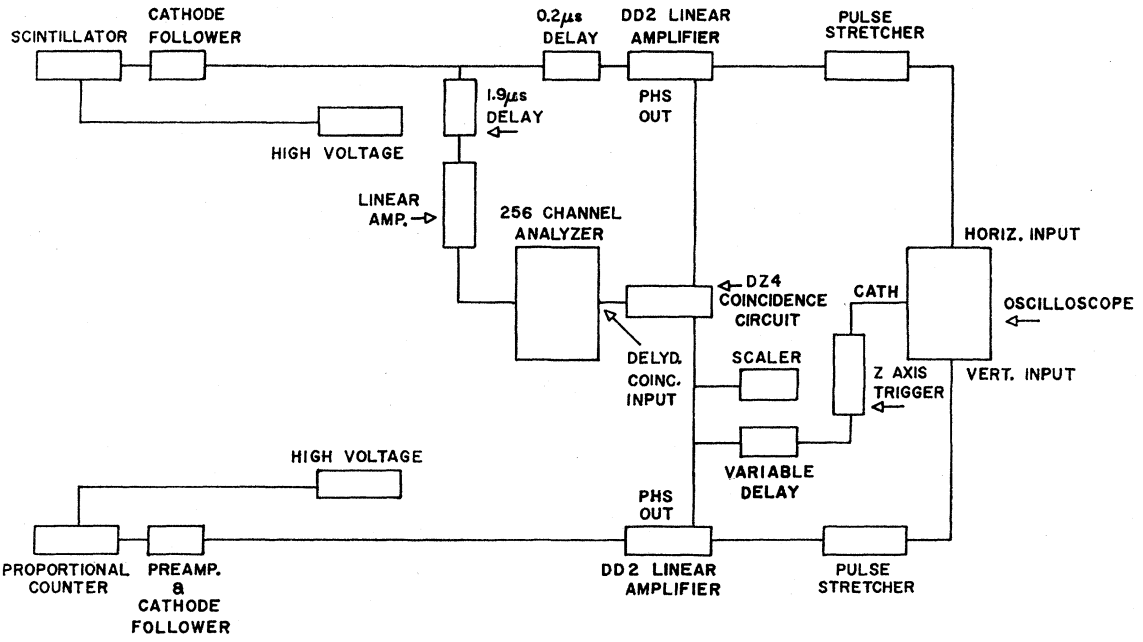

FIG. 1. Block diagram of electronics used with the detection system.

multiplication system. The remaining distributions were obtained by constructing a composite of energy spectra taken with two PHS level settings.

In order to determine the proper PHS level settings, which vary with target thickness and atomic number, it is convenient to have some visual check of the particle distributions and energies. A visual monitor was provided by separately amplifying and flattening pulses from each of the detectors and subsequently applying these signals to the vertical and horizontal inputs of an oscilloscope.[7] The oscillocsope trace was brightened by a signal triggered from the PHS associated with the (dE/dX) counter during the flat part of the shaped detector pulses. The result of this arrangement was to display, as single points on the oscilloscope screen, the locations of all particles being selected for analysis in terms of the coordinates (dE/dX) vs E. This plot was then photographed by Polaroid camera for the purpose of a detailed inspection.

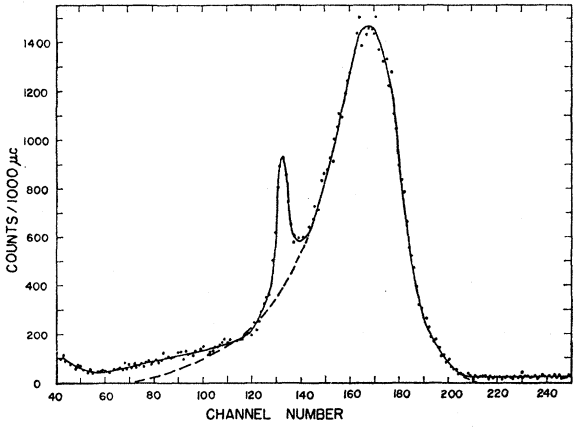

FIG. 2. Energy spectrum for Au at 90°. This is a typical example of unprocessed data recorded on the 256-channel analyzer using the detection system described in the text. Data of this type were used in constructing the surveys shown in figures 4–8.

A typical example of unprocessed data is shown in Fig. 2. The sharp peak occurring at channel 130 is the result of "leakage" of elastic deuteron pulses through the particle separation system. Since this effect is related to the intensity of the elastic deuteron peak, the leakage becomes rather fierce at low scattering angles and completely overrides the alpha spectra for targets of high atomic number. Because of this effect, no data have been presented for elements of $Z>50$ at the lowest scattering angle (30°).

The nonlinear response of CsI to alphas made it necessary to perform an energy calibration of the system. This was accomplished by measuring the pulse-height distributions for natural alpha sources and for (d,α) reactions having well-known Q values. The resulting calibration curve is shown in Fig. 3.

Loss of counts through analyzer dead time was minimized by reducing count rates by controlling the cyclotron beam intensity. The incident beam current was adjusted, so that a reduction of intensity by a factor of 5 would result in less than a 10% variation in the number of counts in a peak.

Over-all accuracy of the final energy spectra (in the center-of-mass system) was judged to be ±0.3 Mev. Energy resolution varied between 8% at 8 Mev and 5% at 23 Mev. Relative cross sections have been assigned an error of ±15%; errors in absolute cross sections are less than 25%.

TABLE I. List of targets and thicknesses.

Target material	Thickness (mg/cm²)	Target material	Thickness (mg/cm²)
Bi	7.0	Sn^{124}	7.1
Pb	9.2	In	6.6
Au	7.3	Cd	4.2
Pt	8.7	Ag	3.3
Ta	14.7	Pd	5.1
Er	8.6	Rh	6.6
Nd	2.4	Nb	13.2
Pr	2.1	Zr	7.0
CsI	10.0	Zn	2.8
To	7.2	Cu	3.0
Sb^{116}	5.5	Ni	0.49
Sn^{117}	6.9	F^{19} (Teflon)	1.4
Sn^{118}	7.3	C^{12}	0.6
Sn^{119}	7.3	C^{13}	0.6
Sn^{120}	7.1	Be	4.2
Sn^{122}	7.1	...	...

Energy distributions for each target were recorded at least twice at any given scattering angle. The position and resolution of the deuteron elastic peak was carefully measured between successive runs as a check on possible gain and resolution shifts in the detection system and electronics.

A list of targets used and their thicknesses is given in Table I. In the majority of cases, targets used were commercially available metal foils. Targets of Er, Te, and Sb were made by evaporating the material on a tantalum or stainless steel plate and peeling off the accumulated deposit in the form of a self-supporting sheet.

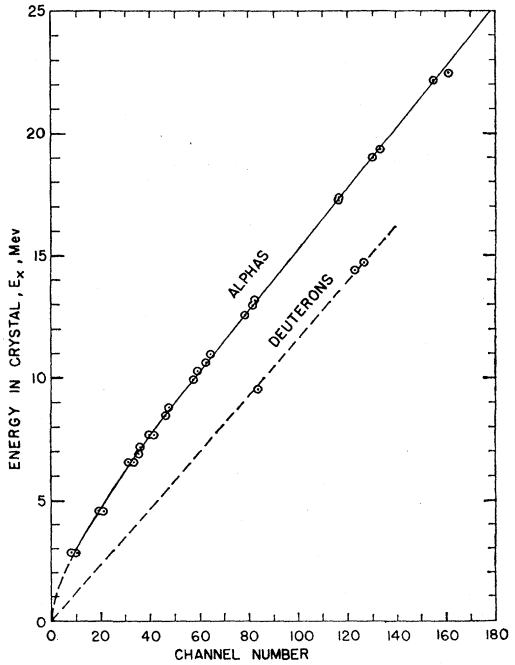

FIG. 3. Crystal calibration curve. The points were obtained with pulse-height distributions resulting from (d,α) reactions on Be^9, C^{12}, C^{13}, Al^{27}, and F^{19}; and with natural alphas from Po^{212} and Bi^{212}.

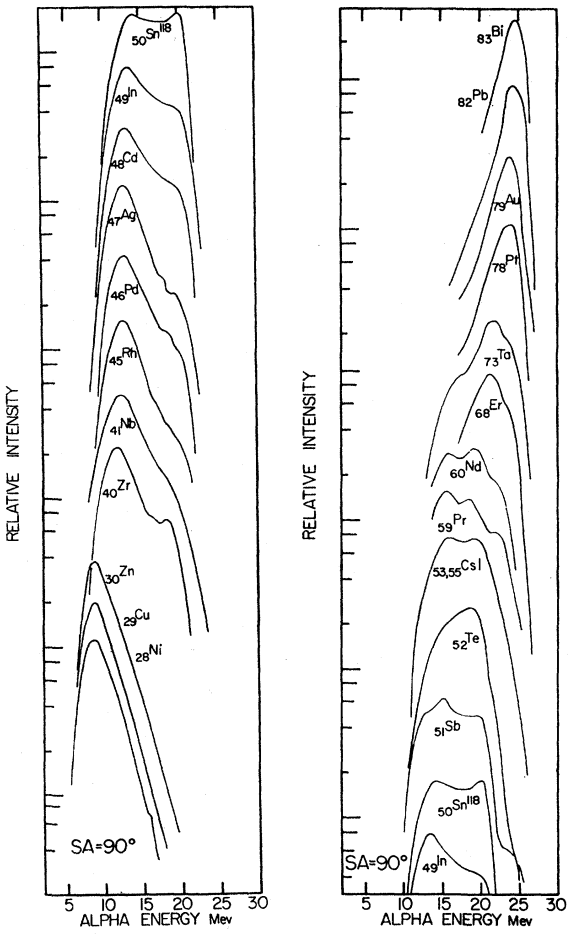

FIG. 4. Low-resolution survey of energy spectra from (d,α) reactions at 90°. Energies are given in the center-of-mass system.

RESULTS AND ANALYSIS

Energy spectra in the center-of-mass system are shown for the scattering angles 90°, 60°, 30°, and 120° in Figs. 4 through 7. Experimental values for the absolute differential cross sections integrated over the energy spectra are given in Table II.

The two outstanding features of the spectra are the appearance of two strong groups which vary regularly with atomic number, and the similarity of the structure at different scattering angles.

The differential cross section at 90° falls off rapidly by a factor of 22 between $_{29}$Cu and $_{50}$Sn. This decrease is associated with the rapid disappearance of the low-energy group around $Z=50$. At this point, the distribution consists predominantly of the high-energy group which has a relatively constant cross section as a function of mass number.

Variation of the energy distributions with angles for four elements is shown in Fig. 8. These nuclei are representative of different regions the periodic table covered. Although relative intensities change, the peaks show little or no energy shift with angle.

TABLE II. Differential cross sections in mb/sr as a function of scattering angle.

Element	120°	90°	60°	30°
Ni	6.6	7.3	7.7	10.0
Cu	···	6.5	7.8	12.0
Zn	···	5.6	7.7	10.0
Zr	0.63	1.0	1.5	3.0
Nb	···	1.4	1.7	3.7
Rh	0.86	1.1	1.5	2.6
Pd	0.53	0.82	1.1	2.2
Ag	0.79	1.0	1.5	2.6
Cd	0.39	0.58	0.98	2.1
In	0.30	0.52	0.84	1.7
Sn^{118}	0.19	0.33	0.71	1.5
Sb	0.23	0.37	···	···
Te	···	0.27	···	···
Er	0.18	0.23	0.38	3.0
Ta	···	0.20	···	···
Pt	···	0.17	0.29	···
Au	0.14	0.20	0.31	1.5
Pb	···	0.27	0.37	···

A. Low-Energy Peak

The peak of the low-energy group shifts in energy with atomic number from 8.5 Mev at $_{29}$Cu to 12.5 Mev at $_{45}$Rh. For $Z\sim30$ the angular distributions show rather weak forward peaking, i.e., isotropy with scattering angle, a characteristic of the compound-nucleus model. In the region of $_{45}$Rh there is a somewhat stronger forward rise in the intensity of the low-energy peak, probably indicating an admixture of alpha particles originating from a direct-reaction mechanism.

The peak energies and angular distributions agree qualitatively with previous results for[10,11] (p,α) and[12] (α,α') scattering which fit the statistical model. This suggests an interpretation of the behavior of the low-energy group based upon statistical theory. Accordingly, determinations of the nuclear temperature and level density parameter were made from the energy distributions and used to compute the compound-nucleus cross sections which in turn were compared to the experimentally observed cross sections.

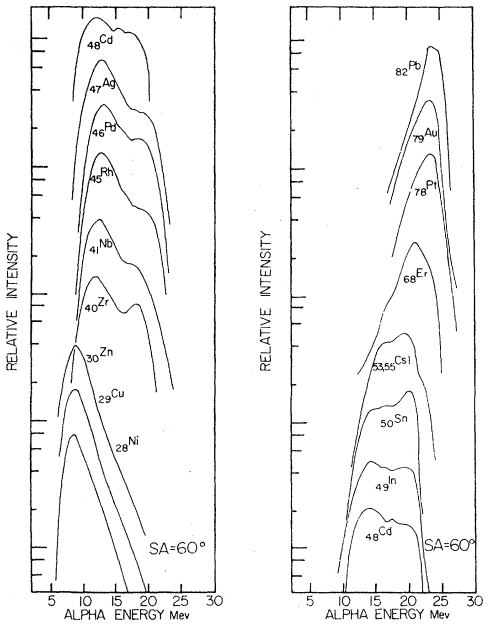

FIG. 5. Low-resolution survey energy spectra from (d,α) reactions at 60°.

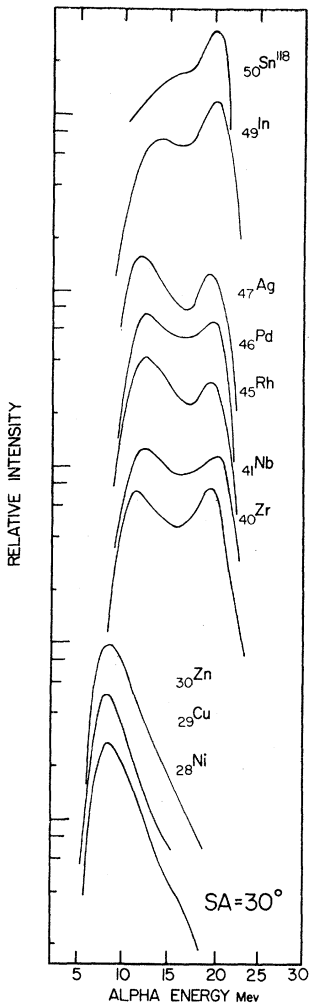

FIG. 6. Low-resolution survey of energy spectra from (d,α) reactions at 30°.

The energy distribution predicted by statistical theory is given[13] by

$$N(\epsilon) \propto \epsilon\sigma_c(\epsilon)\omega(E), \qquad (1)$$

where ϵ is the total disintegration energy (alpha+recoil) in the c.m. system, $\sigma_c(\epsilon)$ is the inverse capture cross section (including Coulomb effects) for the residual

[10] C. B. Fulmer and B. L. Cohen, Phys. Rev. **112**, 1672 (1958).
[11] R. Sherr and F. P. Brady, *Proceedings of the University of Pittsburgh Conference on Nuclear Structure*, edited by S. Meshkov (University of Pittsburgh and Office of Ordnance Research, U. S. Army, 1957), p. 376.
[12] H. W. Fulbright, N. O. Lassen, and N. O. R. Poulsen, Kql. Danske Videnskab. Selskab. Mat fys. Medd. **31**, No. 10 (1959).
[13] J. M. Blatt and V. P. Weisskopf, *Theoretical Nuclear Physics* (John Wiley & Sons, Inc., New York, 1952).

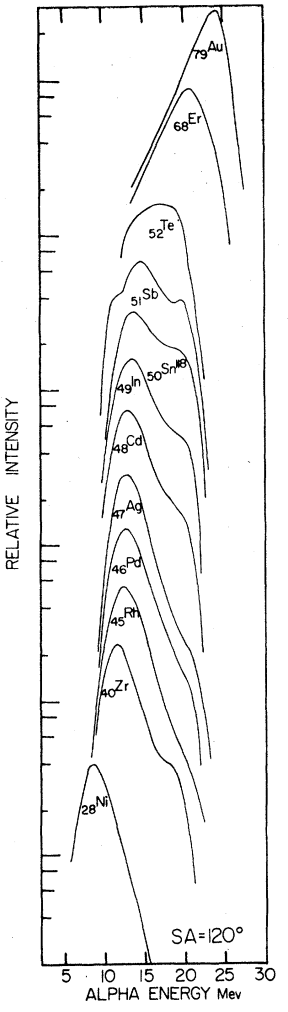

FIG. 7. Low-resolution survey of energy spectra from (d,α) reactions at 120°.

nucleus, and $\omega(E)$ is a measure of the final nuclear level density in terms of the excitation energy E.

Taking the logarithm of both sides of (1) and differentiating, one obtains

$$\frac{d}{dE}\left(\ln\frac{N(\epsilon)}{\epsilon\sigma_c(\epsilon)}\right)=\frac{d}{dE}\ln\omega(E)=\frac{1}{T(E)}, \qquad (2)$$

where $T(E)$, the nuclear temperature, is defined by the last of (2) in analogy with the statistical mechanical definition of temperature[13]. It is commonly assumed[13] that

$$\omega(E)=C\exp[2(aE)^{\frac{1}{2}}], \qquad (3)$$

where a in known as the level density parameter; taking logarithms and differentiating, one gets

$$\frac{d}{dE}\ln\omega(E)=(a/E)^{\frac{1}{2}}. \qquad (4)$$

Thus if the measured energy spectrum—$N(\epsilon)$ vs ϵ—is converted to a plot of $\ln[N(\epsilon)/\epsilon\sigma_c(\epsilon)]$ vs E, the slope of this plot gives a determination of T from (2) and of a from (2) and (4).

TABLE III. Values of statistical model parameters determined from energy spectra.

Nucleus	Excitation Energy (Mev)	$T(90°)$ (Mev)	$T(120°)$ (Mev)	$a(90°)$ $(\text{Mev})^{-1}$	$a(120°)$ $(\text{Mev})^{-1}$
Ni	9.8	1.28	1.33	6.0	5.5
Cu	11.4	1.18	···	8.2	···
Zn	11.0	1.25	···	7.0	···
Zr	8.4	1.27	1.31	5.0	4.9
Nb	11.1	1.44	···	5.4	···
Rh	9.9	1.24	1.22	6.4	6.7
Pd	8.7	1.26	1.26	5.5	5.5

The inverse cross section, σ_c, was taken from the results of experiments in which alpha particles bombard nuclei; a survey of these is given in reference 10.[14] They correspond to the calculations presented by Blatt and Weisskopf[13] for $r_0\simeq 1.6$ f. The effective excitation energy, E, was corrected for pairing effects by the method of Cameron.[15] Values for T and a were extracted for all nuclei where the direct-interaction (DI) contribution to the low-energy portion of the spectrum was judged to be small enough not to interfere appreciably. The determinations were made at an energy well below the DI region, but well above the region where Coulomb barrier penetration predominantly influences the shape of the spectrum.

Results for the nuclear temperature and level density parameter are presented in Table III. Values of a determined from the energy distributions appear to be

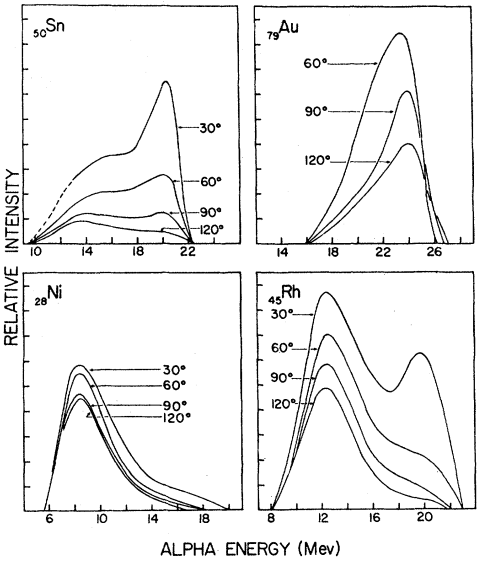

FIG. 8. Variation of energy distributions with scattering angle. These nuclei are representative of different regions of the periodic table covered.

[14] See also F. S. Houck and J. M. Miller, Phys. Rev. **123**, 231 (1961).

[15] A. G. W. Cameron, Can. J. Phys. **36**, 1040 (1958).

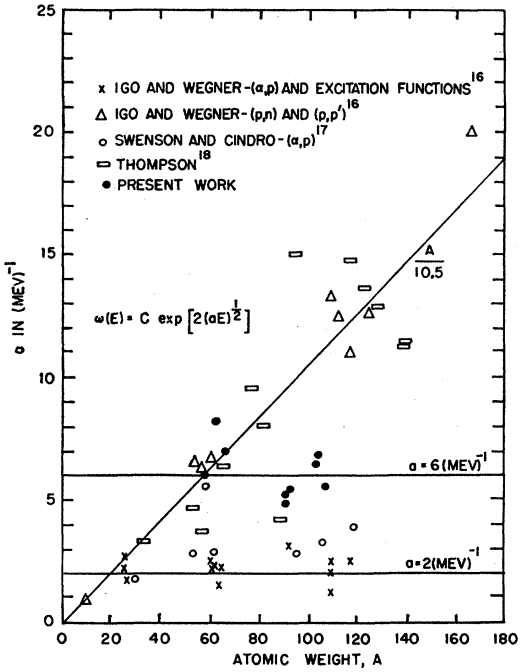

FIG. 9. Comparison of level density parameters for various experiments.

almost independent of atomic weight, in contradiction to the Fermi gas model which predicts a linear variation of a with atomic weight. A similar constant behavior of a has been found previously by other workers[16,17] from (α,p) reactions. Comparison of these data with the present work is presented in Fig. 9.[18] Level density parameters determined from (p,p'), (p,n), and (n,n') reactions at 18 and 150 Mev show clustering about the line $a=A/10.5$ Mev^{-1}. On the other hand, (α,p) experiments at 40 Mev and excitation function experiments induced by gamma rays, neutrons, and alphas tend to give the constant value $a=2$ Mev^{-1} from $A=25$ to 120. The present (d,α) work indicates a tendency towards the somewhat higher value: $a=6$ Mev^{-1}.

A possible explanation suggested by the data for this phenomenon is the presence of the increasing percentage of direct interaction near $_{45}$Rh, even at large scattering angles, as evidenced in Figs. 4 and 7. The effects on the nuclear temperatures through the energy distributions would be to depress the values of the level density parameter a in the regions of higher atomic number, thus suggesting that a spurious value for a has been determined. Although this is possible, it seems unlikely since the general trend of the observed compound-nucleus cross section in the region from $_{29}$Cu to $_{50}$Sn fits the calculated cross section better for $a=$constant than for a linear variation of a with A, as shown below.

[16] G. Igo and H. E. Wegner, Phys. Rev. **102**, 1364 (1956).
[17] L. W. Swenson and N. Cindro, Bull. Am. Phys. Soc. **5**, 76 (1960).
[18] D. B. Thompson, thesis, Los Alamos Scientific Laboratory, 1960 (unpublished).

In Fig. 10, the experimental cross sections, corrected for direct-interaction effects by subjective estimation, have been plotted as a function of atomic number. These were calculated using the 90° data only, and assuming the compound-nucleus angular distributions to be isotropic. Connecting lines were added for the sake of clarity. The relationship for calculating the cross section is given by[13]

$$\sigma(d,\alpha)=\sigma_c(d)\frac{f_\alpha}{\sum_i f_i},$$
$$f_i=g_i m_i\int_0^{E_i}\epsilon\sigma_c(\epsilon)\exp\{2[a(E_i-\epsilon)]^{\frac{1}{2}}\}d\epsilon. \tag{5}$$

Although element-to-element fluctuations in the cross sections are poorly reproduced, the over-all variation with atomic number agrees well with statistical theory for a constant. The calculated compound-nucleus cross section for Au is less than 0.05 mb/sr. This readily explains the absence of a compound-nucleus (CN) peak in this region.

Absolute values for the cross section appear to fit the data better for $a=10$ Mev^{-1} than for $a=5.2$, the latter being closer to the experimentally determined value of the level density parameter. It should be emphasized that in view of the approximations involved in the theory and the sensitivity of the calculations to Coulomb barrier effects (dependent on the choice of

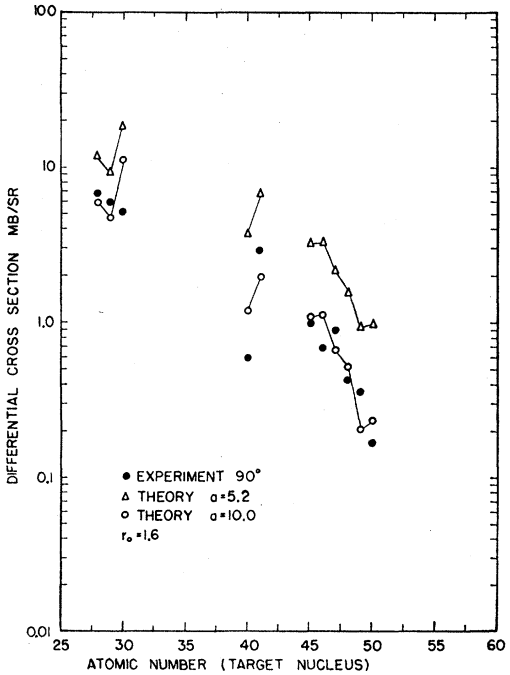

FIG. 10. Comparison of experimental cross sections for the low-energy peak with theoretical calculations which assume a compound-nucleus process and use statistical theory of nuclear reactions.

TABLE IV. Comparison of calculated and observed relative cross sections in the tin isotopes. Calculations use $a=5.2$, but the results are very insensitive to a.

Nucleus	$d\sigma/d\Omega$ (observed)	$d\sigma/d\Omega$ (calculated)
Sn^{116}	100	100
Sn^{117}	70	50
Sn^{118}	29	31
Sn^{119}	32	32
Sn^{120}	19	20
Sn^{122}	12.7	9
Sn^{124}	6.4	5

radius parameter), agreement of absolute cross sections with theory is not expected, and quantitative conclusions based upon this agreement (e.g., values for r_0) are questionable.

The isotopes of Sn provide a good test for statistical theory independent of Coulomb effects. Since the nuclear charge is fixed, and the radius parameter remains constant over the relatively narrow span of mass number ($\Delta A=8$), Coulomb effects are not expected to contribute strongly to variations in relative cross sections. In making theoretical calculations, it is also found that variations in the level density parameter do not greatly influence the relative cross sections. Accordingly, in the competition between different reactions (d,n), (d,p), and (d,α), the strong dependence on Q values becomes the dominating factor.

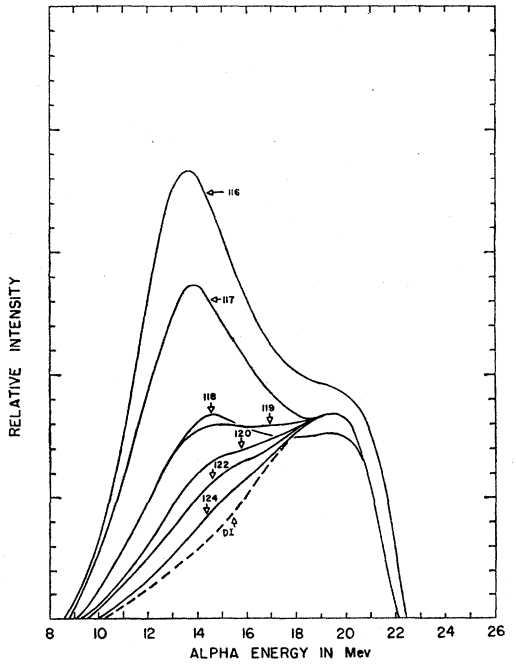

FIG. 11. Energy distributions for Sn isotopes, $\theta_L=90°$. Detailed variations between the different isotopes near the high-energy peak have been averaged to avoid confusion. An estimation of the amount of direct interaction present is shown by the dashed line.

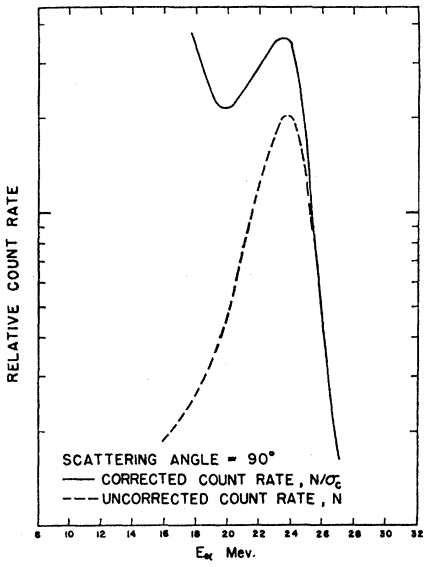

FIG. 12. Coulomb correction for Au spectrum. The persistence of the peak after correction indicates that the low-energy falloff is not due primarily to Coulomb effects.

Energy distributions were obtained for seven separated isotopes of tin: mass numbers 116, 117, 118, 119, 120, 122, and 124. The results are shown in Fig. 11 along with an estimated curve for the amount of direct interaction present. This estimation was based on the shape of the energy distributions observed at higher atomic number where DI effects appear to dominate the spectrum.

Observed relative cross sections were obtained by measuring the remaining peak height after subtraction of the DI curve. These values, normalized to a cross section of 100 for Sn^{116}, are compared to calculated cross sections for $r_0=1.6$ f, $a=5.2$ Mev^{-1} in Table IV. The close agreement lends very strong support to a compound-nucleus description for the low-energy peak.

B. High-Energy Peak

The energy distribution, especially in the region from Pt to Bi, is characterized by a sharply peaked maximum which falls rapidly on the high-energy side and somewhat more slowly with decreasing energy. The salient features of this group are as follows:

(1) These peaks, although quite narrow (~5 Mev), are very much wider than the instrumental resolution indicating that a group of states is excited. When Coulomb corrections are made, the low-energy falloff is found not to be due to a Coulomb barrier cutoff. An example is illustrated in Fig. 12 for Au. The uncorrected energy spectrum has been plotted (broken line) on a log scale in comparison with the spectrum corrected for Coulomb effects (solid line). The corrections were accomplished by dividing the count rate, N, by the capture cross section, σ_c, which is essentially the Coulomb barrier penetration factor. The persistence of

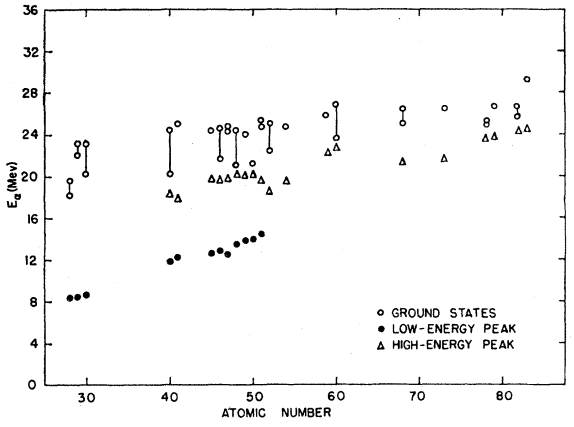

FIG. 13. Comparison of peak energies with predicted ground-state transition energies. Vertical lines show the range of ground-state energies among the various isotopes of polyisotopic targets. Where the energy varies slightly with angle, an average is taken.

the peak on the corrected curve indicates that the fall-off is not a Coulomb effect.

(2) There is a slow, regular variation in the peak energy with atomic number; this is shown in Fig. 13, which includes a plot of the position of this peak vs atomic number. Data for the seven isotopes of Sn also suggest that only small shifts in the peak energy are present (see Fig. 11).

(3) Strong forward peaking occurs in the angular distribution for the high-energy group. This effect, usually associated with direct interactions, is clearly seen in Fig. 8.

(4) The positions of both high- and low-energy groups have been compared with ground-state transition energies in Fig. 13. From this plot it is evident that ground states are weakly excited for all nuclei investigated. There also seems to be no correlation between energies of ground states and the high-energy peaks. This rules out the possibility that the peaks are due to the excitation of collective states, as the latter occur at *excitation energies* that vary slowly with mass number.

(5) There are no strong odd-even differences in peak energies between adjacent nuclei. This is also observed in the tin isotopes (see Fig. 11).

Two widely considered reaction mechanisms can be suggested to explain the results: (1) a knockout process, (2) a pickup mechanism. The arguments against the knockout process have been discussed in reference 5 and will not be included here. On the other hand, a "pickup" or inverse stripping mechanism can readily explain the most outstanding features of the experimental results, as will now be shown.

The neutron and proton would most easily be picked up from single-particle states in the major shell that is filling. These states are closely grouped in energy, and this energy depends only on the size of the potential well which varies slowly with mass number. These ideas, in conjunction with a stripping mechanism, have been successfully used to explain a similar regular structure found in (d,p) reactions.[19]

First we consider an even-even nucleus. In general, there are about five substates for each major shell in the region of interest. In accordance with pairing theory,[20] these subshells are pair-filled by an amount proportional to their occupation numbers, V^2. If the proton and neutron substates are given the designation A_i and B_j, respectively, (d,α) reactions would be expected to excite single-particle states of the form $(A_i)^{-1}(B_j)^{-1}$ with strengths related to the occupation numbers for A_i and B_j. Out of the 25 possible states of this form, one will be the ground state. Assuming crudely equal probabilities for exciting any given state, the ground state should on the average be excited only about 4% of the time.

The approximate energy interval from the ground state to the centroid of all the states is expected to be about twice the average excitation energy of single-particle states. These energies are not inconsistent with the 1- to 2-Mev excitations observed in the data.

For odd-A target nuclei, the situation is somewhat different. An additional unpaired nucleon is present (in a state A_k). There are then two types of states excited in (d,α) reactions: (a) those of the form $(A_k)^1(A_i)^{-1}(B_j)^{-1}$ and (b) those having the configuration $(A_k)^0(B_j)^{-1}$, one of which is the ground state. The binding energies for the latter type are larger than those for the former by an amount about equal to the energy gap in even-even nuclei (2–3 Mev). Furthermore, the Q value for (d,α) reactions leading to states of type (a) should be about the same as for (d,α) reactions in even-even nuclei, as both require the breaking of a neutron pair and a proton pair. Thus one expects the energy spectrum of alpha particles from (d,α) reactions on odd-mass target nuclei to contain two peaks—one (which we designate peak B) due to levels of type (b) which includes the ground state and is centered at 1–2 Mev excitation energy, and one (peak A) due to levels of type (a) which is centered at 3–5 Mev excitation energy, and at the same Q value as the peak in even-even nuclei. Let us consider the expected relative intensities of these two peaks:

In the first place, peak A includes about four times as many states (20 vs 5 in our example), so that it should be four times larger on this account. In addition, one must consider the fact that pickup reaction cross sections are proportional to fractional parentage coefficients, $S(if)$.

For the configuration j^n, French[21] has shown that

$$S(n,n-1)=n, \qquad (n \text{ even})$$
$$=1-[(n-1)/(2j+1)], \qquad (n \text{ odd}).$$

[19] B. L. Cohen, J. B. Mead, R. Price, K. Quisenberry, and C. Martz, Phys. Rev. **118**, 499 (1960).

[20] L. S. Kisslinger and R. A. Sorensen, Kql. Danske Videnskab. Selskab. Mat. fys. Medd. **32**, No. 9 (1960).

[21] J. B. French, *Nuclear Spectroscopy—Part B*, edited by F. Ajzenberg-Selove (Academic Press Inc., New York, 1960).

Thus S is very much smaller for (d,α) reactions leading to states of type (b) for which n is odd, than for those leading to states of type (a) for which n is even. For example, for $j=5/2$, $n=3$ gives $S=0.67$ whereas $n=4$ gives $S=4.0$. Thus, peak A is larger than peak B by a factor of $4\times4.0/0.67$ (the first factor of 4 is from the number of levels, considered above) $=24$. Thus it is not surprising that only peak A is prominent in the experimental results, and the spectra are very similar for odd- and even-mass nuclei.

V. CONCLUSION

Of the two strong alpha-particle groups observed in the energy spectra, the low-energy peak was found to be predominantly a compound-nucleus evaporation effect and to be in good agreement with the predictions of statistical theory. The principal features of the high-energy peak can be explained by a two-particle pickup process which involves the removal of nucleons from combinations of single-particle states in the filling major shells.

There are, however, additional features of the energy distributions that cannot be easily explained. For instance, the triple peak observed in Pr and Nd. These peaks are not the result of a mixture of isotopes, since Pr is mono-isotopic. A tendency towards double peaking in the energy spectra is also apparent for the elements Er and Te. These features appear to be isolated parts of a systematic trend for these regions. At the time of data accumulation, few targets were available for these ranges of nuclei, and large intervals in atomic number could not be studied.

A more thorough understanding of the nature of the high-energy peak can only be obtained with higher resolution experiments. At present such a program is under way utilizing diffused junction solid-state detectors and mono-isotopic targets. The results of this study will be presented in a forthcoming article.

ACKNOWLEDGMENTS

The authors wish to express their appreciation to Dr. Elizabeth Baranger, Dr. Karl Quisenberry and Dr. Allen G. Blair for helpful discussions and suggestion concerning certain phases of this work. They are indebted to William Stewart and John DeFrancesco for invaluable assistance in making calculations and in the collection and processing of data. They wish to thank the members of the cyclotron staff and machine shop personnel for their cooperation. Special thanks are due Mr. George Fodor for preparing and mounting most of the targets used in this experiment and to Mr. Johannes Bakker for his assistance in solving many electronics problems.

The authors also wish to thank Dr. A. J. Allen and acknowledge the financial support given by the joint program of the Office of Naval Research and the U. S. Atomic Energy Commission and by the National Science Foundation.

PHYSICAL REVIEW VOLUME 125, NUMBER 3 FEBRUARY 1, 1962

Neutron Giant Resonances—Nuclear Ramsauer Effect*

J. M. PETERSON
Lawrence Radiation Laboratory, University of California, Livermore, California and Institute for Theoretical Physics, Copenhagen, Denmark

(Received July 31, 1961)

Three continuous families of broad maxima and minima are observed in neutron total cross sections between 0.1 and 100 Mev. All shift smoothly to higher energy with increasing mass number. The relationships among the families, their energy-mass number dependence, and their detailed locations can be understood in terms of a semiclassical treatment of a simplified optical model. The oscillations are seen to result from interference between the part of the neutron wave which has traversed the nucleus with the part which has gone around. This nuclear situation is analogous to the Ramsauer effect in electron interactions with noble gases. An alternative explanation of the broad maxima as due to resonances of single partial waves is not valid because in general several partial waves are simultaneously important and because the partial wave characteristics change rapidly as one traverses a continuous family of maxima. The widths of the broad maxima are related more to the parameters of the real potential well than to the depth of the imaginary potential well.

I. INTRODUCTION

THE curves of neutron total cross section versus energy often show broad maxima in the energy region of a few Mev and higher. These maxima are illustrated in Fig. 1. Before the measurements were made it had been expected on theoretical grounds that the variation with energy would be a simple monotonic decrease—something like $2\pi(R+\lambda\!\!\!^{-})^2$, R being the nuclear radius and $\lambda\!\!\!^{-}$ the neutron wavelength divided by 2π. The theoretical model[1] here was that the nucleus was black to neutrons. Note that on the average this model gave

* The work described in this report was initiated at the Lawrence Radiation Laboratory, University of California, and completed in its final form at the Institute for Theoretical Physics, Copenhagen, Denmark. It was supported by the U. S. Atomic Energy Commission.

[1] H. Feshbach and V. F. Weisskopf, Phys. Rev. **76**, 1550 (1949).